MODELING OF ELECTROMECHANICAL SYSTEMS BASED ON INDUCTION MACHINE USING METHOD OF AVERAGE VOLTAGE ON THE INTEGRATION STEP LENGTH

Oleksiy KUZNYETSOV[1]

Numerical models of induction machine were designed using the method of average voltage on the integration step length. Calculation time, numerical integration steps that provide given value of error and the boundaries of stability for numerical models of induction machine based on this method were compared with those using conventional methods of numerical integration. It was concluded that method of average voltage on the integration step length provides increasing the integration step length with sufficient accuracy. Application of the first-order method allows to reduce the calculation time by 30%. Therefore it is advantageous to apply the method for designing the high-speed models of electromechanical systems based on induction machine.

Keywords: induction machine, mathematical model, method of average voltage on the integration step length

1. Introduction

Real-time operation of numerical models is a necessary condition to provide the interaction between the objects of the real world and virtual objects. Most of powerful simulators widely used in electromechanical, power and energy tasks, like Matlab/Simulink, VisSim or LabView use the techniques that can provide a natural time scale of simulated processes. The examples of such kind of simulators in electrical engineering are [1] and [2] for Matlab/Simulink or [3] for LabView. Those simulators allow applying their code to FPGA or microprocessors ([3], [4], [5]). At the same time approaches like [6] are based on direct hardware programming without using simulators.

The general considerations of the real-time systems and their application in power system simulation is given in [7]. The paper [8] describes different real-time techniques used in electric systems and drives. A state-of-the-art and comprehensive analysis of contemporary real-time simulation platforms is widely discussed in [9]. The paper distinguishes four main industrial real-time simulators: RTDS, eMEGAsim, HYPERSIM and VTB. All of them provide an operation in hybrid models.

[1]Associate professor, Department of Electromechanics and Electronics, Hetman Petro Sahaidachnyi National Army Academy, Lviv, Ukraine, e-mail: oleksiy.kuznyetsov@ukr.net

Present paper focuses on designing high-speed numerical models of the electromechanical systems (EMS) based on induction machine (IM) for real-time application. Different approaches on designing real-time models of IM and EMS on their base can be found in [3], [10], [11], [12], [13]).

In this regard a method of average voltage on an integration step length (AVSL), presented for the first time in [14], is interesting for high-speed and real-time applications. The paper [15] compares AVSL with conventional methods of numerical integration for DC and AC circuit computation, in particular, with those used in Matlab/Simulink. It was stated that the methods providing highest operation speed with equal errors are:

- the third-order AVSL,
- the fourth-order Adams-Bashforth method,
- the fourth-order Adams-Moulton method and
- the second-order AVSL.

The program environment of EMS modeling based on object-oriented method for analysis of EMS [16] using AVSL was designed under supervising of prof. O. Plakhtyna. The results of that work were published in [17] for EMS based on IM and in [18] for EMS based on synchronous machines. The principles of that environment operation were first stated in [19]: the model of EMS is formed by the models of separate objects represented as electrical multiport networks and the incidence matrices that determine the way of networks' connections.

Therefore, the scope of the present research work is defined as discovering the purposes of applying AVSL for the tasks of designing a high-speed models of EMS based on IM.

2. Modeling an EMS based on IM using AVSL

2.1. General description of the method

The AVSL essence can be explained on an electrical circuit branch with applied voltage u on its terminals, containing electromotive force e, resistance R, inductance L and capacitance C connected in series. According to [14] an electrical balance on the integration step length Δt with initial point t_0 can be written as

$$U + E - U_R - U_C - U_L = 0, \tag{1}$$

where $U = \frac{1}{\Delta t}\int_{t_0}^{t_0+\Delta t} u\,\mathrm{d}t$, $E = \frac{1}{\Delta t}\int_{t_0}^{t_0+\Delta t} e\,\mathrm{d}t$, $U_R = \frac{1}{\Delta t}\int_{t_0}^{t_0+\Delta t} u_R\,\mathrm{d}t$, $U_C = \frac{1}{\Delta t}\int_{t_0}^{t_0+\Delta t} u_C\,\mathrm{d}t$, $U_L = \frac{1}{\Delta t}(\psi_1 - \psi_0)$ are average values of applied voltage and voltages on appropriate branch elements on an integration step length; ψ_0 and ψ_1 are flux linkages on the initial and final point of the step, respectively.

If current curve on the integration step length is depicted as m-order polynomial, then an equation (1) according to [14] is written after voltage drops on resistance and on capacitor in an initial point of the step u_{R0} and u_{C0}, respectively, as follows:

$$U+E-u_{R0}-u_{C0}+\left(\frac{R}{m+1}+\frac{\Delta t}{C}\cdot\frac{2-(m+1)(m+2)}{2(m+1)(m+2)}+\frac{L_0}{\Delta t}\right)i_0-$$
$$-\sum_{k=1}^{m-1}\left(\frac{R\Delta t^k}{(k+1)!}\cdot\frac{m-k}{m+1}+\frac{\Delta t^{k+1}}{C(k+2)!}\cdot\frac{(m+1)(m+2)-(k+1)(k+2)}{(m+1)(m+2)}\right)\cdot \tag{2}$$
$$\cdot\frac{\mathrm{d}^{(k)}i_0}{\mathrm{d}t^{(k)}}-\left(\frac{R}{m+1}+\frac{\Delta t}{C(m+1)(m+2)}+\frac{L_1}{\Delta t}\right)i_1=0,$$

Unknown values in (2) are:

- current in the final point of the step i_1 and
- average applied voltage on an integration step length U.

2.2. IM equations using AVSL

According to [19] IM is represented as twelve-port electrical network (Fig. 1). Thus IM is represented in phase coordinates on the supposition that magnetic field in air gap is sinusoidally distributed, motor parameters remain constant, iron losses are equal to zero, currents in slot conductors are uniform, and mechanical losses are equal to zero so that torque on motor's shaft is equal to electromagnetic torque. However, representing IM in phase coordinates allows taking into consideration the winding asymmetry.

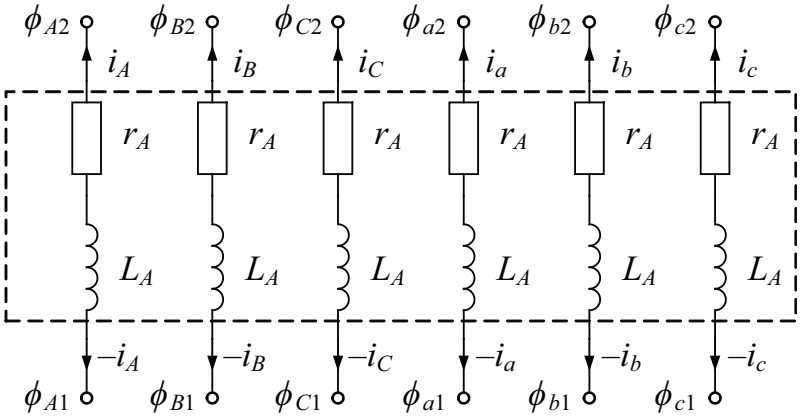

Fig. 1. Computational scheme of IM

Therefore, the equation (2) for IM is written in matrix form as

$$\frac{1}{\Delta t}\int_{t_0}^{t_0+\Delta t}\boldsymbol{\phi}_1\,\mathrm{d}t-\frac{1}{\Delta t}\int_{t_0}^{t_0+\Delta t}\boldsymbol{\phi}_2\,\mathrm{d}t+\mathbf{R}_m\,\mathbf{i}_{m0}-\frac{\mathbf{R}_m}{m+1}\mathbf{i}_{m0}-$$
$$-\sum_{k=1}^{m-1}\frac{\mathbf{R}_m\Delta t^k}{(k+1)!}\cdot\frac{m-k}{m+1}\cdot\frac{\mathrm{d}^{(k)}\mathbf{i}_{m0}}{\mathrm{d}t^{(k)}}-\frac{\mathbf{R}_m}{m+1}\mathbf{i}_{m1}-\frac{1}{\Delta t}(\boldsymbol{\psi}_{m1}-\boldsymbol{\psi}_{m0})=0, \tag{3}$$

where:

$\boldsymbol{\phi}_1 = [\phi_{A1}, \phi_{B1}, \phi_{C1}, \phi_{a1}, \phi_{b1}, \phi_{c1}]^T$ and $\boldsymbol{\phi}_2 = [\phi_{A2}, \phi_{B2}, \phi_{C2}, \phi_{a2}, \phi_{b2}, \phi_{c2}]^T$ are potentials' vectors of IM represented as Fig. 1,

$\mathbf{i}_{m0} = [i_{A0}, i_{B0}, i_{C0}, i_{a0}, i_{b0}, i_{c0}]^T$ is a vector of currents in outer branches of electric network (vector of stator and rotor currents) in an initial point of step, and

$\mathbf{i}_{m1} = [i_{A1}, i_{B1}, i_{C1}, i_{a1}, i_{b1}, i_{c1}]^T$ is a vector of the same currents in a final point of step,

$\mathbf{R}_m = diag\,[r_A, r_B, r_C, r_a, r_b, r_c]$ is a matrix of windings' resistances,

$\boldsymbol{\psi}_{m0} = [\psi_{A0}, \psi_{B0}, \psi_{C0}, \psi_{a0}, \psi_{b0}, \psi_{c0}]^T = \mathbf{L}_m \mathbf{i}_{m0}$ and

$\boldsymbol{\psi}_{m1} = [\psi_{A1}, \psi_{B1}, \psi_{C1}, \psi_{a1}, \psi_{b1}, \psi_{c1}]^T = \mathbf{L}_m \mathbf{i}_{m1}$ are vectors of windings' flux linkage in an initial and in a final point of the step, accordingly, $\mathbf{L}_m$ is a matrix of self and mutual inductances of the machine:

$$\mathbf{L}_m = \begin{bmatrix} L_{AA} & L_{AB} & L_{AC} & L_{Aa} & L_{Ab} & L_{Ac} \\ L_{BA} & L_{BB} & L_{BC} & L_{Ba} & L_{Bb} & L_{Bc} \\ L_{CA} & L_{CB} & L_{CC} & L_{Ca} & L_{Cb} & L_{Cc} \\ L_{aA} & L_{aB} & L_{aC} & L_{aa} & L_{ab} & L_{ac} \\ L_{bA} & L_{bB} & L_{bC} & L_{ba} & L_{bb} & L_{bc} \\ L_{cA} & L_{cB} & L_{cC} & L_{ca} & L_{cb} & L_{cc} \end{bmatrix}.$$

Thereafter the equation (3) is written as:

$$\begin{aligned} &\frac{1}{\Delta t}\int_{t_0}^{t_0+\Delta t} \boldsymbol{\phi}_1\,\mathrm{d}t - \frac{1}{\Delta t}\int_{t_0}^{t_0+\Delta t} \boldsymbol{\phi}_2\,\mathrm{d}t + \mathbf{R}_m \mathbf{i}_{m0} - \frac{\mathbf{R}_m}{m+1}\mathbf{i}_{m0} - \\ &- \sum_{k=1}^{m-1} \frac{\mathbf{R}_m \Delta t^k}{(k+1)!} \cdot \frac{m-k}{m+1} \cdot \frac{\mathrm{d}^{(k)}\mathbf{i}_{m0}}{\mathrm{d}t^{(k)}} - \frac{\mathbf{R}_m}{m+1}\mathbf{i}_{m1} - \frac{1}{\Delta t}\mathbf{L}_m \mathbf{i}_{m1} + \frac{1}{\Delta t}\mathbf{L}_m \mathbf{i}_{m0} = 0, \end{aligned} \tag{4}$$

where unknown values are currents in outer branches in the final point of step $\mathbf{i}_{m1}$.

According to [14] each branch of multiport in Fig. 1 on an integration step length is represented as connected in series equivalent stepper electromotive force E_s and equivalent stepper branch resistance R_s with a current i_{m1} flowing through the branch. Thus (4) is written as

$$\frac{1}{\Delta t}\int_{t_0}^{t_0+\Delta t} \boldsymbol{\phi}_1\,\mathrm{d}t - \frac{1}{\Delta t}\int_{t_0}^{t_0+\Delta t} \boldsymbol{\phi}_2\,\mathrm{d}t - \mathbf{R}_s \mathbf{i}_{m1} - \mathbf{e}_s = 0, \tag{5}$$

where the vector of stepper electromotive force $\mathbf{e}_s$ and the matrix of stepper branch resistances $\mathbf{R}_s$ are specified as follows:

$$\mathbf{R}_s = \frac{\mathbf{R}_m}{m+1} + \frac{1}{\Delta t}\mathbf{L}_m, \tag{6}$$

and

$$\mathbf{e}_s = \frac{m\,\mathbf{R}_m}{m+1}\mathbf{i}_{m0} + \sum_{k=1}^{m-1} \frac{\mathbf{R}_m \Delta t^k}{(k+1)!} \cdot \frac{m-k}{m+1} \cdot \frac{\mathrm{d}^{(k)}\mathbf{i}_{m0}}{\mathrm{d}t^{(k)}} - \frac{1}{\Delta t}\mathbf{L}_m \mathbf{i}_{m0} = 0. \tag{7}$$

Taking (6) and (7) into consideration, the equation (5) is written in a form presented in [19]:

$$\mathbf{i}_1 + \mathbf{G}_m \int_{t_0}^{t_0+\Delta t} \boldsymbol{\phi}_m \, \mathrm{d}t + \mathbf{c}_m = 0, \tag{8}$$

where $\mathbf{i}_1 = [\mathbf{i}_{m1}, -\mathbf{i}_{m1}]^T$, $\boldsymbol{\phi}_m = [\boldsymbol{\phi}_1, \boldsymbol{\phi}_2]^T$,

$\mathbf{G}_m = \begin{bmatrix} \mathbf{R}_s^{-1} & -\mathbf{R}_s^{-1} \\ -\mathbf{R}_s^{-1} & \mathbf{R}_s^{-1} \end{bmatrix}$ and $\mathbf{c}_m = \begin{bmatrix} \mathbf{R}_s^{-1} \\ -\mathbf{R}_s^{-1} \end{bmatrix} \times \mathbf{e}_s$.

To complete a mathematical model of IM using AVSL one should also include the equations

$$\omega_{m1} = \omega_{m0} + \frac{T_e - T_l}{J} \Delta t, \tag{9}$$

and

$$\gamma_{m1} = \gamma_{m0} + z_p \, \omega_{m0} \, \Delta t, \tag{10}$$

where T_e is average electromagnetic torque on a step length, T_l is average load torque on a step length, J is rotor inertia, z_p is number of pole pairs. In (9)

$$T_e = \frac{3}{2} z_p L_\mu \left(i_{r\beta} i_{s\alpha} - i_{r\alpha} i_{s\beta} \right), \tag{11}$$

where $i_{s\alpha}$, $i_{s\beta}$, $i_{r\alpha}$, $i_{r\beta}$ are stator and rotor currents in (α, β) reference frame, L_μ is magnetizing inductance. When considering the effect of saturation, L_μ is a function of magnetizing current.

Therefore, the equations (8)–(11) mold the mathematical model of IM using AVSL.

2.3. Generating the model of EMS

The model of EMS is generated according to the method presented in [19], and developed in [17] and [18] for AVSL. In this case EMS is considered as a combination of basic elements presented as electric networks. Each element is described by terminal matrix equation

$$\mathbf{i}_e + \mathbf{G}_e \int_{t_0}^{t_0+\Delta t} \boldsymbol{\phi}_e \, \mathrm{d}t + \mathbf{c}_e = 0, \tag{12}$$

where $\mathbf{i}_e$ is a vector of currents in outer branches, $\boldsymbol{\phi}_e$ is a vector of potentials of outer terminals, $\mathbf{G}_e$ and $\mathbf{c}_e$ are matrix and vector defined after an element structure, respectively.

To generate a model of the system as a whole one has to connect networks with their terminals. The dependence between the potentials of elements' terminals $\boldsymbol{\phi}_e$ and the potentials of system's nodes $\boldsymbol{\phi}_s$ is written as

$$\frac{1}{\Delta t} \int_{t_0}^{t_0+\Delta t} \boldsymbol{\phi}_e \, \mathrm{d}t = \boldsymbol{\Pi}_e^T \frac{1}{\Delta t} \int_{t_0}^{t_0+\Delta t} \boldsymbol{\phi}_s \, \mathrm{d}t, \tag{13}$$

where the incidence matrices $\boldsymbol{\Pi}_e$ define the way of interconnection between the EMS elements.

To define the vector of average system nodes' potentials on the step length $\int_{t_0}^{t_0+\Delta t} \boldsymbol{\phi}_s \, \mathrm{d}t$ on each step of numerical integration one has to solve the matrix equation

$$\mathbf{G}_s \int_{t_0}^{t_0+\Delta t} \boldsymbol{\phi}_s \, \mathrm{d}t + \mathbf{c}_s = 0. \tag{14}$$

$\mathbf{G}_s$ and $\mathbf{c}_s$ in (14) are matrix and vector of nodal matrix equation:

$$\mathbf{G}_s = \sum_{j=1}^{k} \boldsymbol{\Pi}_j \, \mathbf{G}_{ej} \, \boldsymbol{\Pi}_j^T \quad \text{and} \quad \mathbf{c}_s = \sum_{j=1}^{k} \boldsymbol{\Pi}_j \, \mathbf{c}_{ej} \tag{15}$$

where $\mathbf{G}_{ej}$ and $\mathbf{c}_{ej}$ are the coefficients of matrix nodal equation (12) for each of j EMS elements (here $j = 1, 2, \ldots, k$, where k is the quantity of EMS elements).

With average nodes' potentials on a step length for each element one has to determine the average system nodes' potentials on a step length according to (13). Then the currents of elements' outer branches in final point of a step are defined from the equation (12).

3. **Materials and methods**

Numerical and computer models of the system Power Network–IM were created using the number of numerical integration methods such as:

- second-order Runge-Kutta method (RK2) as recommended in [16] because of its sufficient result accuracy while small amount of calculations,
- fourth-order Adams-Bashforth (AB4) and fourth-order Adams-Moulton (AM4) methods: provide the best operation speed and accuracy for modeling electric circuits, according to [15],
- first and second-order AVSL (AVSL1 and AVSL2).

Computer model of IM using the AVSL2 passed verification in [17], where waveforms obtained on experimental unit were compared with simulation results. The standard deviation between both results was less than 6%. The detailed description of the verification is presented in [17].

Five computer models mentioned above were used for simulation an IM direct start mode with different values of integration step starting with 10^{-6} sec up to the stability boundaries of each method. Parameters of the machine applied in that models are presented in Appendix. Note, that L_μ is assumed to be constant here.

With an amount of integration step 10^{-6} sec the deviation between simulation results obtained on all computer models (speed, electromagnetic torque, stator and rotor currents) was not above the level of $10^{-3}\%$, while for most variables the level of deviation was $10^{-6}\%$.

The way of calculating the accuracy of the methods used in [15] was to compare the result of the modeling with an analytical solution. However, it is impossible to obtain the analytical solution of IM equations. Therefore, we consider the simulation results obtained using the step 10^{-6} sec to be a *standard* (Fig. 2). So, all the simulation results obtained have to be compared with that *standard* values.

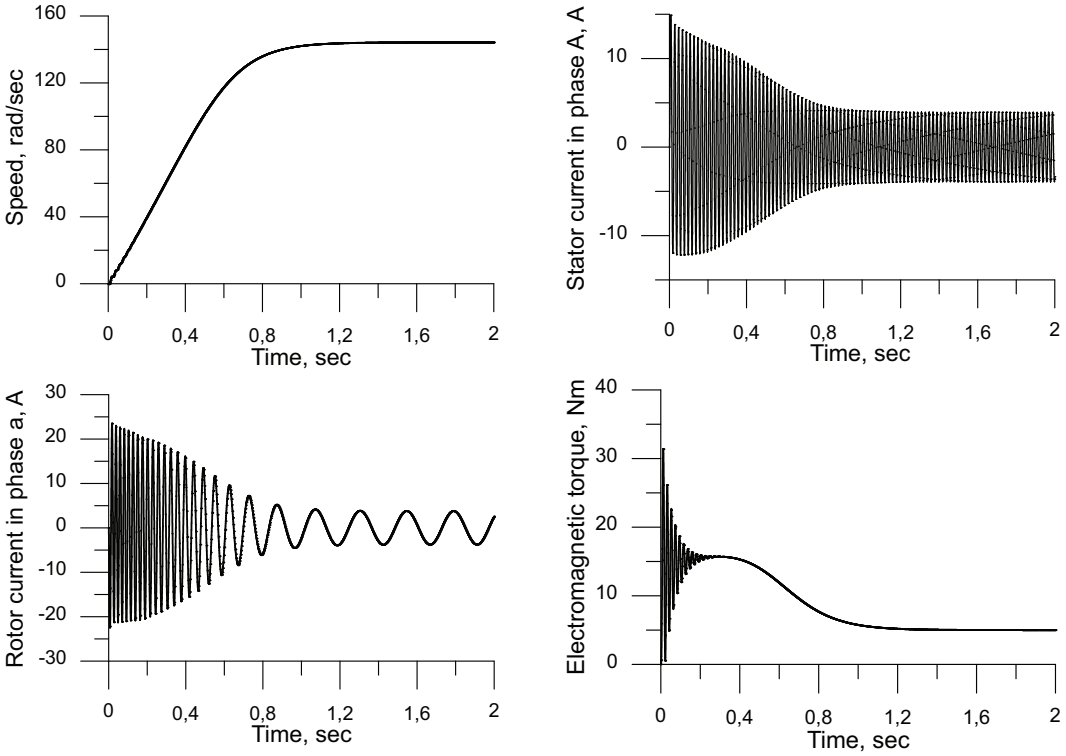

Fig. 2. *Standard* simulation results

4. **Experimental part and discussion**

4.1. **Operation speed of the models**

A comparison of simulation results obtained on five computer models using step 10^{-6} sec stated that difference between the duration of calculation for computer models using the Adams methods and AVSL2 was less than 2% (thus for AB4 and AM4-based computer models the duration was 150 sec and 149 sec, respectively, and 153 sec for AVSL2-based computer model). For RK2-based computer model the duration of calculation was 158 s. As a result, the difference between all those values do not exceed 8%. Application of AVSL1 allows increasing the operation speed by 30% (up to 90 s).

Actually, the analysis of the equation (2) shows that m-order AVSL requires information about the derivatives up to $(m-1)$ order. So, AVSL1-based model does not require derivatives calculation, AVSL2-based model requires first order derivative calculation, AVSL3-based model requires an information about first and second order derivatives, and so on. It means that increasing the order of the method demands increasing the number of calculation and their duration.

4.2. Accuracy and stability boundaries of the methods

The next experiment was held while enlarging the step value. Simulation result obtained in that case was compared with *standard* results for each point being calculated. So, each variable x is characterized by an average error referred to steady state value:

$$\delta_x = \frac{1}{N} \cdot \frac{\sum_{i=1}^{N} |x_{std}(t_i) - x_{calc}(t_i)|}{|x_{ss}|} \cdot 100\%, \tag{16}$$

where $x_{std}(t_i)$ is a standard value in a time point t_i (in i point of calculation), $x_{calc}(t_i)$ is a value in the same point of time being calculated using the computer model based on one of the methods mentioned above with the given step value, x_{ss} is a value of x in steady state, or amplitude in steady state for periodical variables, N is the number of calculation points.

However, the frequency of rotor current is a function of slip. It results in the next significant feature as it is shown in Fig. 3. The figure depicts simulation results obtained on all models mentioned above using the step length 10^{-3} sec together with *standard* results (only AB4 is unstable with this step value). *Standard* speed waveform is particularly the same as waveforms obtained on AM4 and AVSL2-based models.

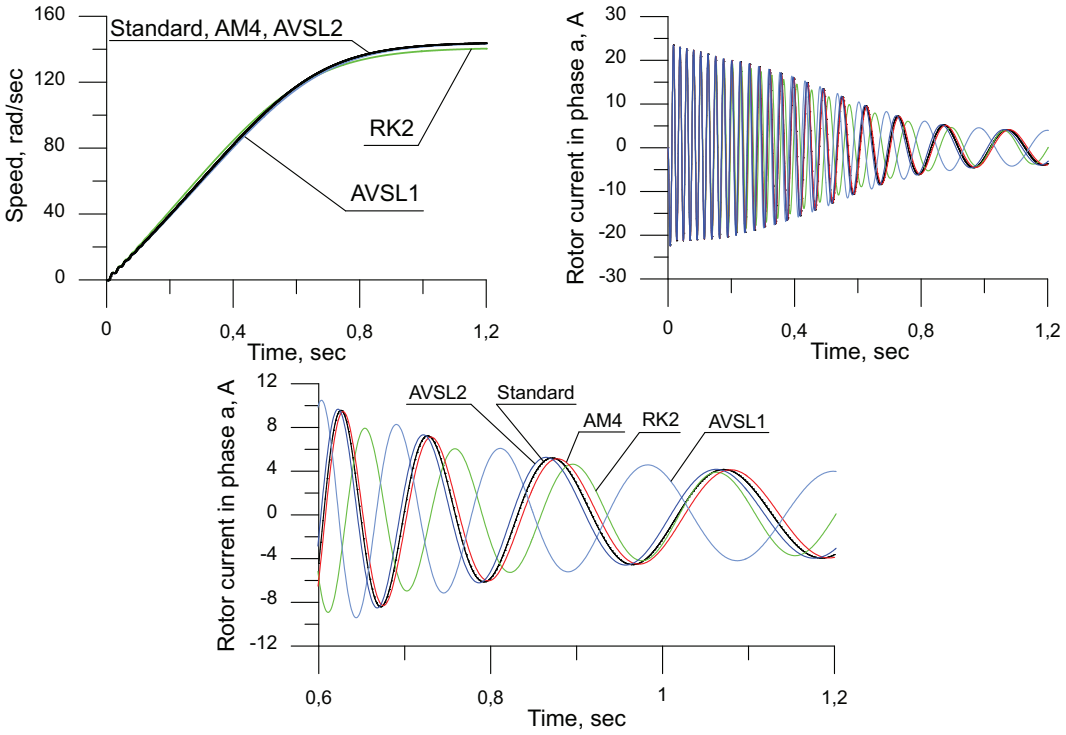

Fig. 3. Simulation results using step 1×10^{-3} sec

The waveforms of speed obtained on RK2-based model differ both in transient and in steady state. It results in less then 7% envelope deviation of the rotor current, together with frequency and amplitude deviation in steady state. The speed waveform calculated on AVSL1-based model differs only in transient. It results in difference in rotor current initial phase in steady state while an amplitude and frequency are the same. So, envelope deviation in transient is near 1%.

Similarly, Fig. 4 shows the simulation results obtained using the step length of 1.5×10^{-3} s. Waveform deviation obtained on RK2-based model increases in comparison with that obtained previously. Thus, the results shown in Fig. 4 are satisfied for all the models but AB4-based model. However, according to (16) error levels of rotor current are as follows: 140% in AVSL1-based model and 110% in RK2-based model.

Therefore, it is preferable to take into account the general behavior of the functions in the way of comparing not the instantaneous values but waveforms and envelopes for periodical variables. In this case for each variable $x_{calc}(t_i)$ integrals calculated as:

$$S_x = \sum_{i=1}^{N} |x_{calc}(t_i)| \, \Delta t \tag{17}$$

were compared with that to standard value S_{xstd}. Thus while an equation (16) was used to calculate an error for instantaneous values, (17) shows error for integral assessment.

The step length that provides maximum relative error at the level of 1%, 5% and 10% for all the models was defined according to equations (16) and (17). The results are given in the Table. Also it contains maximum step value when each method loses its stability. Note that the lowest amount of all the time constants of IM is 7.05×10^{-2} s.

Table 1

Experimental results

Maximum relative error		Integration step, s				
		RK2	AM4	AB4	AVSL1	AVSL2
for instantaneous values	1%	$4.5 \cdot 10^{-5}$	$5.95 \cdot 10^{-4}$	$3.2 \cdot 10^{-4}$	$3 \cdot 10^{-5}$	$4.5 \cdot 10^{-5}$
	5%	$1.1 \cdot 10^{-4}$	$6 \cdot 10^{-4}$	$\approxeq 3.2 \cdot 10^{-4}$	$1.1 \cdot 10^{-4}$	$1.7 \cdot 10^{-4}$
	10%	$1.5 \cdot 10^{-4}$	$9.3 \cdot 10^{-4}$	$\approxeq 3.2 \cdot 10^{-4}$	$1.7 \cdot 10^{-4}$	$4.5 \cdot 10^{-4}$
for integral assessment	1%	$5 \cdot 10^{-4}$	$\approxeq 1.45 \cdot 10^{-3}$	$\approxeq 3.2 \cdot 10^{-4}$	$1 \cdot 10^{-3}$	$4 \cdot 10^{-3}$
	5%	$9 \cdot 10^{-4}$	$\approxeq 1.45 \cdot 10^{-3}$	$\approxeq 3.2 \cdot 10^{-4}$	$2.2 \cdot 10^{-3}$	$9 \cdot 10^{-3}$
	10%	$1.1 \cdot 10^{-3}$	$\approxeq 1.45 \cdot 10^{-3}$	$\approxeq 3.2 \cdot 10^{-4}$	$3 \cdot 10^{-3}$	$1.1 \cdot 10^{-2}$
Maximum step value		$2 \cdot 10^{-3}$	$1.45 \cdot 10^{-3}$	$3.21 \cdot 10^{-4}$	$8 \cdot 10^{-3}$	$2 \cdot 10^{-2}$

Analyzing the first part of the table one can state that the lowest accuracies for instantaneous values are when using RK2 and AVSL1-based models. The best accuracy is obtained using the fourth order Adams methods (that confirms [15]).

At the same time more informative is the second part of the table. Thus high accuracy of the fourth-order Adams methods (not above 1% for integral assessment) is provided in stability regions of these methods. Actually, the special feature of

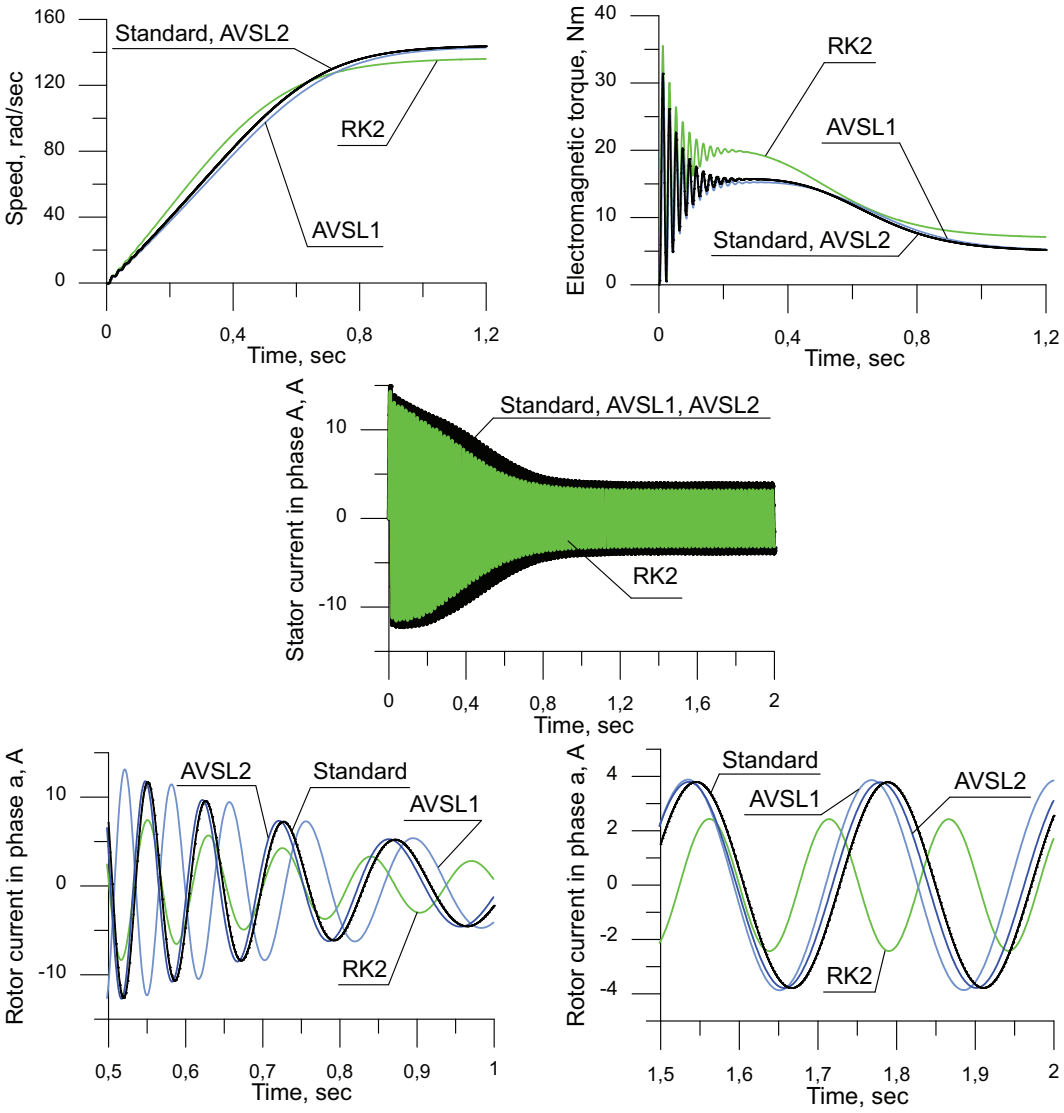

Fig. 4. Simulation results using step 1.5×10^{-3} sec

Adams methods is their ability not to accumulate error [20]. Nevertheless, AVSL's feature is the widest stability region.

5. Conclusions

The equations of induction machine have been written using the method of average voltages on the step length. Behavior of this method was compared in the case of modeling EMS based on induction machine with behavior of those methods of numerical integration having advantages in modeling DC and AC circuits. These methods are second-order Runge-Kutta method, and fourth-order Adams-Bashforth and Adams-Moulton methods.

It has been stated that the best accuracy for instantaneous values can be obtained using fourth-order Adams methods. However, the method of average voltages on the step length provides the widest stability region, and allows increasing the step while satisfactory error range. Also, using the first-order method of average voltages on the step length allows reducing the calculation time by 30%. Therefore it is advantageous to apply the method of average voltages on the step length for designing the high-speed models of electromechanical systems based on induction machine.

Appendix

Machine parameters: $R_s = 7.32\ \Omega$, $L_{\sigma s} = 0.0146$ H, $R_r = 3.0\ \Omega$, $L_{\sigma r} = 0.0418$ H, $L_\mu = 0.2696$ H, $J = 0.05$ kg m^2 (All rotor parameters are referred to stator with transformation variable $k_{trans} = 2$).

Abbreviations

AB4	fourth-order Adams-Bashforth method
AM4	fourth-order Adams-Moulton method
AVSL	method of average voltage on the step length
AVSL1	first-order method of average voltage on the step length
AVSL2	second-order method of average voltage on the step length
EMS	electromechanical system
IM	induction machine
RK2	second-order Runge-Kutta method

REFERENCES

[1] *S. Abourida and J. Bélanger*, "Real-Time Platform for the Control Prototyping and Simulation of Power Electronics and Motor Drives", in Proc. of the Third International Conference on Modeling, Simulation and Applied Optimization (ICSMAO), Sharjah (U.A.E.), Jan. 20-22, 2009, pp. 1-6.

[2] *S. Umashankar, M. Bhalekar, S. Chandra, D. Vijayakumar, and D. P. Kothari*, "Development of a New Research Platform for Electrical Drive System Modelling for Real-Time Digital Simulation Applications", in Advances in Power Electronics, **vol. 2013**, Article ID 719847, 2013, 10 pages, (DOI 10.1155/2013/719847).

[3] *P. Ponce, L. Ibarra, A. Molina, and B. MacCleery*, "Real Time Simulation for DC and AC Motors Based on LabView FPGAs", in Information Control Problems in Manufacturing, **vol. 14**, no. 1, May 2014, pp. 1777-1784.

[4] *M. Dagbagi, A. Hemdani, L. Idkhajine, M. W. Naouar, E. Monmasson, and I. Slama-Belkhodja*, "ADC-Based Embedded Real-Time Simulator of a Power Converter Implemented in a Low-Cost FPGA: Application to a Fault-Tolerant Control of a Grid-Connected Voltage-Source Rectifier" in IEEE Transactions on Industrial Electronics, **vol. 63**, no. 2, Feb. 2016, pp. 1179-1190, (DOI 10.1109/TIE.2015.2491883)

[5] *S. Karimi, A. Gaillard, P. Poure, and S. Saadate*, "FPGA-Based Real-Time Power Converter Failure Diagnosis for Wind Energy Conversion Systems", in IEEE Transactions on Industrial Electronics, **vol. 55**, no. 12, Dec. 2008, pp. 4299-4308, (DOI 10.1109/TIE.2008.2005244)

[6] *M. Baszyński*, "Low cost, high accuracy real-time simulation used for rapid prototyping and testing control algorithms on example of BLDC motor", in Archives of Electrical Engineering, **vol. 65(3)**, 2016, pp. 463-479. (DOI 10.1515/aee-2016-0034)

[7] *P. Venne, J.-N. Paquin, and J. Bélanger* "The What, Where and Why of Real-Time Simulation", in Planet RT, Oct. 2010.

[8] *P. M. Menghal and A. J. Laxmi*, "Real time control of electrical machine drives: A review", in 2010 International Conference on Power, Control and Embedded Systems (ICPCES), Allahabad, 2010, pp. 1-6. (DOI 10.1109/ICPCES.2010.5698697)

[9] *M. D. Omar Faruque et al.*, "Real-Time Simulation Technologies for Power Systems Design, Testing, and Analysis", in IEEE Power and Energy Technology Systems Journal, **vol. 2**, no. 2, pp. 63-73, June 2015, (DOI 10.1109/JPETS.2015.2427370)

[10] *B. Asghari and V. Dinavahi*, "Permeance network based real-time induction machine model", in Proc. IPST, Kyoto, Japan, 2009.

[11] *R. Magureanu, B. Popa, H. Hedesiu, and F. Hurdoi*, "FPGA Real-Time Simulation of the Squirrel Cage Induction Generators Used for Conversion of Renewables" in Proceedings of the Xth Edition of The Annual Conference The Academic Days of The Academy of Technical Sciences in Romania, Galati, 2015, pp. 222-225.

[12] *A. Derouich, Ahmed Lagrioui, and Moulay Ismail*, "Real-Time Simulation and Analysis of the Induction Machine Performances Operating at Flux Constant", International Journal of Advanced Computer Science and Applications, **vol. 5**, iss. 4, 2014, pp. 59-64 (DOI 10.14569/IJACSA.2014.050410)

[13] *L. Charaabi*, "FPGA-Based Fixed Point Implementation of a Real-Time Induction Motor Emulator", in Advances in Power Electronics, **vol. 2012**, Article ID 409671, 2012, 10 pages, (DOI 10.1155/2012/409671).

[14] *O. Plakhtyna*, "Numerical One-Step Method of Electric Circuits Analysis and Its Application in Electromechanical Tasks" (in Ukrainian), in Visnyk Natsionalnoho Tekhnichnoho Universytetu "Kharkivskyi politekhnichnyi instytut", 2008, **vol. 30**, pp. 223-225.

[15] *Z. Kłosowski, O. Plakhtyna, and P. Grugel*, "Applying the Method of Average Voltage on the Integration Step Length for the Analysis of Electrical Circuits", in Zeszyty Naukowe, Elektrotechnika 17, **vol. 264** Bydgoszcz, 2014, pp. 17-31.

[16] *A. Kutsyk*, "Object-Oriented Method for Analysis of Electromechanical Systems" (in Ukrainian), in Technical electrodynamics, **vol. 2**, Kyiv, 2006, pp. 57-63.

[17] *O. Plakhtyna and O. Kuznyetsov*, "The Excitation of the Wound Induction Machine from Capacitor Energy Caused by Slip Power" (in Ukrainian), in Technical electrodynamics, Them. Issue Power Electronic and Energy Efficiency, **vol. 1**, Kyiv, 2010, pp. 153-158.

[18] *O. Plakhtyna, A. Kutsyk, and M. Semenyuk*, "Mathematical Modeling of Electromechanical System with Compensation of Armature Reaction of Synchronous Machine using an Author's Method of Average Voltage on the Integration Step Length" (in Ukrainian), in Technical electrodynamics, Them. Issue Power Electronic and Energy Efficiency, **vol. 2**, Kyiv, 2010, pp. 201-206.

[19] *Ye. Plakhtyna*, Mathematical Modeling of Electromechanical Systems with Semiconductor Converters (in Russian), Vyshcha Shkola, Lvov, 1986.

[20] *I. Babuška, E. Vitásek, and M. Práger*, Numerical Processes in Differential Equations, SNTL, Prague, 1969.